Supplementary Information for

A graphene-like membrane with ultrahigh water flux for desalination

Youguo Yan[a,†], Wensen Wang[a,†], Wen Li[a], Kian Ping Loh[b,c,*] Jun Zhang[a,*]

[a]College of Science, China University of Petroleum, 266580 Qingdao, Shandong, People's Republic of China

[b]Department of Chemistry, National University of Singapore, 3 Science Drive 3, Singapore 117543, Singapore

[c]Centre for Advanced 2D Materials and Graphene Research Centre, National University of Singapore, 6 Science Drive 2, Singapore, 117546, Singapore

Corresponding Author:

Jun Zhang

E-mail: zhangjun.upc@gmail.com

Kian Ping Loh

E-mail: chmlohkp@nus.edu.sg

1. The stable structure and atomic charges of 2D-CAP membrane

The atomic charges of 2D-CAP are obtained by first principle calculations with the B3LYP density functional using Gaussian09.[1,2] In order to obtain the energetically favorable conformation and accurate atomic charge, a model composed of several periodic cells was built to implement calculation (Fig. S1). After simulation, the central cell highlighted by the yellow rectangular panel was selected as the standard periodic cell to eliminate the boundary effect. A supercell using this periodic cell was built to obtain the 2D-CAP membrane in our simulation.

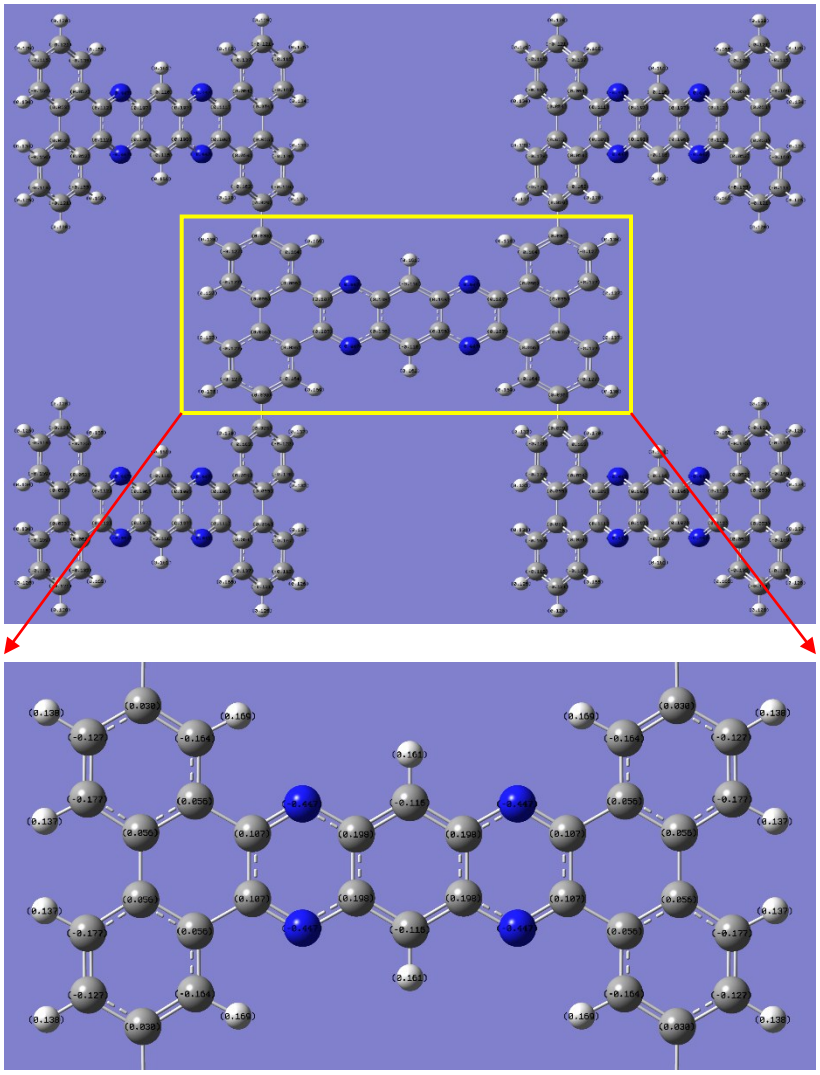

Fig. S1 A structure composed of five periodic cells to implement the first principle calculations, the central cell was selected as the standard periodic cell to build the 2D-CAP membrane in our model

The lattice constants, fractional atomic coordinates and atomic charges could be seen in the Tab. S1.

Tab. S1 Charges used in MD of the 2D-CAP membrane

Element	X	Y	Z	Charges used in MD
C	0.212409	0.924783	0.231167	0.056
C	0.263897	0.883475	0.234823	0.056
C	0.317685	0.924531	0.238267	0.107
C	0.41482	0.92388	0.243342	0.198
C	0.465764	0.883574	0.245104	-0.116
C	0.516904	0.923687	0.246376	0.198
C	0.614032	0.923987	0.24638	0.107
C	0.667775	0.88296	0.24526	0.056
C	0.719381	0.924314	0.243881	0.056
C	0.769376	0.880539	0.242366	-0.177
C	0.768535	0.800934	0.241838	-0.127
C	0.717278	0.759184	0.242935	0.0315
C	0.667733	0.80229	0.244916	-0.164
C	0.263855	0.802858	0.235446	-0.164
C	0.214348	0.75955	0.232139	0.0315
C	0.163095	0.801162	0.227705	-0.127
C	0.162365	0.880932	0.227547	-0.177
C	0.965821	0.383504	0.243359	-0.116
C	0.016922	0.42372	0.242595	0.198
C	0.016881	0.507378	0.243	0.198
C	0.965928	0.547649	0.243972	-0.116
C	0.113921	0.507784	0.239604	0.107
C	0.114033	0.424267	0.239116	0.107
C	0.167814	0.383336	0.236003	0.056
C	0.219385	0.424762	0.234015	0.056
C	0.219153	0.509061	0.234307	0.056
C	0.167358	0.549817	0.237006	0.056
C	0.166667	0.630544	0.236593	-0.164
C	0.216068	0.674183	0.233259	0.0315
C	0.267594	0.633142	0.230995	-0.127
C	0.268903	0.553608	0.231639	-0.177
C	0.269405	0.381039	0.231464	-0.177
C	0.268613	0.301435	0.230424	-0.127
C	0.217384	0.259615	0.231862	0.0315
C	0.167817	0.30267	0.23491	-0.164
C	0.712603	0.508575	0.241202	0.056
C	0.712394	0.424332	0.241412	0.056

C	0.763926	0.383093	0.242505	0.056
C	0.817691	0.424216	0.243025	0.107
C	0.817798	0.507748	0.243235	0.107
C	0.764352	0.549565	0.242529	0.056
C	0.914925	0.507386	0.243986	0.198
C	0.914834	0.423717	0.243671	0.198
C	0.662803	0.552856	0.239773	-0.177
C	0.664124	0.632542	0.240007	-0.127
C	0.715608	0.673802	0.241973	0.0315
C	0.764903	0.63029	0.24304	-0.164
C	0.763961	0.302476	0.243088	-0.164
C	0.714481	0.2591	0.242502	0.0315
C	0.663177	0.30064	0.241278	-0.127
C	0.662374	0.380409	0.240833	-0.177
C	0.212678	0.009031	0.231152	0.056
C	0.317868	0.008079	0.238434	0.107
C	0.264449	0.04997	0.234882	0.056
C	0.414991	0.007556	0.243634	0.198
C	0.51695	0.007342	0.246603	0.198
C	0.466042	0.047719	0.245627	-0.116
C	0.613999	0.007501	0.246501	0.107
C	0.719236	0.008601	0.243682	0.056
C	0.667475	0.049428	0.245311	0.056
C	0.666897	0.130135	0.245125	-0.164
C	0.716252	0.173729	0.242999	0.0315
C	0.767759	0.132628	0.240978	-0.127
C	0.769019	0.053079	0.24144	-0.177
C	0.162894	0.053332	0.227187	-0.177
C	0.164221	0.133004	0.226922	-0.127
C	0.215721	0.174233	0.231036	0.0315
C	0.265002	0.130705	0.234874	-0.164
C	0.270522	0.980798	0.735379	0.056
C	0.322283	0.939963	0.73923	0.056
C	0.375778	0.981872	0.742311	0.107
C	0.472831	0.982036	0.745848	0.198
C	0.523759	0.941675	0.746799	-0.116
C	0.57481	0.981866	0.7467	0.198
C	0.671956	0.981449	0.745078	0.107
C	0.725417	0.939626	0.743768	0.056
C	0.777166	0.980618	0.741988	0.056
C	0.826966	0.936329	0.740484	-0.177
C	0.825649	0.856651	0.740526	-0.127
C	0.774159	0.815394	0.742526	0.0315

C	0.724869	0.858903	0.744148	-0.164
C	0.322858	0.859262	0.739062	-0.164
C	0.273523	0.815678	0.734464	0.0315
C	0.222009	0.856753	0.730842	-0.127
C	0.220742	0.936298	0.731425	-0.177
C	0.023897	0.441761	0.742546	-0.116
C	0.07492	0.482014	0.740938	0.198
C	0.075019	0.565677	0.740914	0.198
C	0.024027	0.605886	0.742633	-0.116
C	0.172163	0.565179	0.736369	0.107
C	0.172055	0.481653	0.736387	0.107
C	0.225515	0.439836	0.733719	0.056
C	0.277264	0.480832	0.731589	0.056
C	0.277463	0.565088	0.731775	0.056
C	0.225922	0.606307	0.733906	0.056
C	0.225858	0.686923	0.734479	-0.164
C	0.275313	0.730325	0.733125	0.0315
C	0.326625	0.688816	0.730542	-0.127
C	0.327466	0.609044	0.729957	-0.177
C	0.327069	0.436535	0.729235	-0.177
C	0.325731	0.356851	0.729278	-0.127
C	0.274234	0.315606	0.731754	0.0315
C	0.224951	0.359123	0.73374	-0.164
C	0.770417	0.564886	0.742176	0.056
C	0.770595	0.480599	0.741944	0.056
C	0.822375	0.439782	0.7431	0.056
C	0.87587	0.481734	0.74373	0.107
C	0.875797	0.56525	0.743967	0.107
C	0.82202	0.606247	0.74362	0.056
C	0.972922	0.565692	0.743635	0.198
C	0.972936	0.482035	0.743527	0.198
C	0.72041	0.608661	0.741114	-0.177
C	0.721243	0.688261	0.741158	-0.127
C	0.772506	0.730018	0.742751	0.0315
C	0.82205	0.686917	0.744306	-0.164
C	0.822931	0.35907	0.743338	-0.164
C	0.773573	0.315481	0.742205	0.0315
C	0.722059	0.356568	0.740768	-0.127
C	0.7208	0.436111	0.740754	-0.177
C	0.270378	0.065095	0.735146	0.056
C	0.375744	0.065379	0.741925	0.107
C	0.321992	0.106418	0.738459	0.056
C	0.472864	0.065696	0.745466	0.198

C	0.574954	0.065539	0.746364	0.198
C	0.523999	0.105819	0.745966	-0.116
C	0.672098	0.064987	0.744806	0.107
C	0.777392	0.064868	0.741764	0.056
C	0.725869	0.106112	0.743299	0.056
C	0.725833	0.186729	0.7436	-0.164
C	0.775307	0.230107	0.74218	0.0315
C	0.826604	0.188557	0.740439	-0.127
C	0.827417	0.108792	0.740396	-0.177
C	0.220398	0.108911	0.731107	-0.177
C	0.221271	0.188512	0.729916	-0.127
C	0.272544	0.230229	0.73296	0.0315
C	0.322062	0.187091	0.737632	-0.164
H	0.46559	0.821293	0.24461	0.161
H	0.809832	0.909038	0.241379	0.137
H	0.808435	0.77101	0.240416	0.138
H	0.627021	0.774855	0.246185	0.169
H	0.304518	0.775387	0.239148	0.169
H	0.12322	0.771142	0.223993	0.138
H	0.12192	0.909372	0.224218	0.137
H	0.965711	0.321219	0.243105	0.161
H	0.965934	0.60995	0.244065	0.161
H	0.125907	0.657578	0.239222	0.169
H	0.307295	0.663494	0.227842	0.138
H	0.309539	0.525599	0.229506	0.137
H	0.309847	0.40958	0.229964	0.137
H	0.308527	0.271547	0.227886	0.138
H	0.12712	0.275204	0.237009	0.169
H	0.622169	0.524777	0.238064	0.137
H	0.624402	0.662796	0.238495	0.138
H	0.805719	0.657502	0.244552	0.169
H	0.804657	0.275047	0.244216	0.169
H	0.623312	0.270578	0.240335	0.138
H	0.621895	0.408786	0.239767	0.137
H	0.466105	0.110021	0.245648	0.161
H	0.626082	0.157183	0.246759	0.169
H	0.807485	0.162938	0.238673	0.138
H	0.809638	0.025017	0.23975	0.137
H	0.122266	0.02526	0.223924	0.137
H	0.124521	0.163282	0.223033	0.138
H	0.305807	0.157933	0.238542	0.169
H	0.523699	0.879376	0.746798	0.161
H	0.867597	0.964407	0.73895	0.137

H	0.865362	0.826385	0.738796	0.138
H	0.684051	0.831694	0.746026	0.169
H	0.363663	0.832218	0.742739	0.169
H	0.182292	0.826436	0.726595	0.138
H	0.180123	0.964352	0.728176	0.137
H	0.023895	0.379457	0.742376	0.161
H	0.024143	0.668162	0.74258	0.161
H	0.185163	0.714327	0.736654	0.169
H	0.366469	0.718918	0.728461	0.138
H	0.367952	0.580686	0.727878	0.137
H	0.367702	0.464606	0.727116	0.137
H	0.365437	0.326564	0.726828	0.138
H	0.184138	0.331923	0.736067	0.169
H	0.679951	0.580154	0.739817	0.137
H	0.681341	0.718183	0.73972	0.138
H	0.862758	0.714347	0.745946	0.169
H	0.863745	0.332003	0.744543	0.169
H	0.682326	0.326262	0.739424	0.138
H	0.680179	0.464173	0.739588	0.137
H	0.524153	0.168101	0.745263	0.161
H	0.685146	0.214155	0.745056	0.169
H	0.866463	0.21863	0.739014	0.138
H	0.867895	0.08041	0.739052	0.137
H	0.179933	0.080436	0.72832	0.137
H	0.18139	0.218456	0.725949	0.138
H	0.362771	0.214507	0.740846	0.169
N	0.365144	0.884381	0.240818	-0.447
N	0.566431	0.883992	0.246655	-0.447
N	0.066237	0.547419	0.241838	-0.447
N	0.066497	0.384145	0.240957	-0.447
N	0.865532	0.547453	0.243877	-0.447
N	0.865186	0.384142	0.243361	-0.447
N	0.365638	0.047703	0.241259	-0.447
N	0.566363	0.047251	0.247002	-0.447
N	0.423423	0.94212	0.744552	-0.447
N	0.624198	0.941779	0.746267	-0.447
N	0.124656	0.605237	0.738777	-0.447
N	0.124315	0.441961	0.73885	-0.447
N	0.923368	0.605303	0.744139	-0.447
N	0.923547	0.442048	0.743833	-0.447
N	0.423342	0.105378	0.743812	-0.447
N	0.624616	0.105078	0.745681	-0.447

2. The method to apply hydraulic pressure

The method to apply hydrostatic pressure on rigid graphene sheets was conducted as follow. To generate the desired pressure (ΔP), the applied force (f) was exerted on each carbon atom of the graphene sheet based on the equation, $f = \Delta P \cdot A / n$,[3,4] where A, n are the area and total number of carbon atoms, respectively. As to different systems, the applied pressure on the left piston sheet changed from 50 to 100 150 and 200 Mpa, while the right piston sheet permanently was applied 0.1 MPa to maintain the water density at 1.0 g/ml.

3. The number of water molecules and Na^+ and Cl^- ions contained in simulation models

Tab. S2 The number of water molecules and Na^+ and Cl^- ions added in feed box

membranes	Hydrostatic pressures											
	50 MPa			100 MPa			150 MPa			200 MPa		
	H_2O	Na^+	Cl^-	H_2O	Na^+	Cl^-	H_2O	Na^+	Cl^-	H_2O	Na^+	Cl^-
1-layer	2500	45	45	6000	108	108	6000	108	108	6000	108	108
2-layer	2500	45	45	5000	90	90	5000	90	90	6000	108	108
3-layer	2500	45	45	4000	72	72	4000	72	72	4000	72	72
4-layer	2500	45	45	3000	54	54	3000	54	54	3000	54	54

Due to the water flux increases with the applied hydrostatic pressure while decreases with the increasing membrane layers, in 6 ns simulation, the total number of passed water molecules in various models is different. To obtain reasonable water flux and ion rejection rate, it is demanded that there are more than half of water molecules in saline box passed into permeate box after simulation.[5] Based on this point, different number of water molecules contained inside the feed box were designed to save computational cost. Meanwhile, to keep identical salt concentration, corresponding number of Na^+ and Cl^- ions were added into the feed box, as shown in Tab. S2. In all model, the permeate box contains 1300 water molecules.

4. Water flux employing different water models

The simulation result adopting TIP4P water model in bilayer membrane was added to compare with the result using SPC water model,[6] the water flux is shown below in Figure R1. It can be seen that there are negligible deviation between these two water flux. This result is added in the revised supplementary material to confirm that the water model has little influence on the water flux in our research.

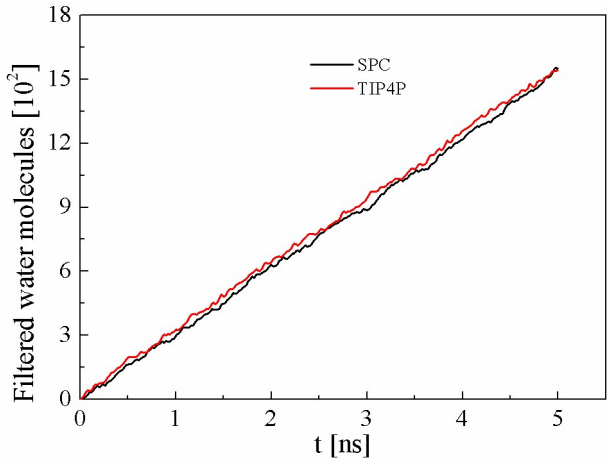

Fig. S2 The water fluxes employing SPC and TIP4P water models in bilayer membrane under hydrostatic pressure of 100 MPa.

5. Lennard-Jones (LJ) parameters

In simulations, the hydrogen and carbon atoms of 2D-CAP were described by the parameterization of benzene by Müller-Plathe et al.,[7] which only includes Lennard-Jones (LJ) parameters for the interactions between each hydrogen and carbon atoms because the coordinates of 2D-CAP were fixed during MD simulation. A similar parameterization drawing from Jorgensen et al.[8] was employed for nitrogen atoms. Waters, Na^+ and Cl^- ions were modeled using the LJ parameters derived by Cheatham et al.[9] and Aluru et al.,[10] respectively. The parameters are summarized in Tab. S3. The inter-atomic LJ parameters between species i and j were calculated using Lorentz-Berthelot mixing rules.

Tab. S3 The charges and Lennard-Jones parameters

Elements	ε (kcal/mol)	σ (Å)	q (e)	References
$C_{2D\text{-}CAP}$	0.0700	3.5500	From Calculation	[7]

$H_{2D\text{-}CAP}$	0.0300	2.4200	From Calculation	[7]
$N_{2D\text{-}CAP}$	0.1700	3.2500	From Calculation	[8]
H_w	0.0000	0.0000	0.4238	[9]
O_w	0.1554	3.1656	-0.8476	[9]
Na^+	0.3526	2.1600	1.0	[10]
Cl^-	0.0128	4.8305	-1.0	[10]

6. The water flux in 20 ns simulation

the water flux of 20 ns simulation in bilayer membrane with hydrostatic pressure of 50 MPa was given in Figure R2. It can be seen that a good linear relationship between the water flow and simulation time is confirmed. The calculated water flux in initial 5 ns and in total 20 ns has negligible deviation, which confirmed the validation of our simulation result. This simulation result has been added in the revised supplementary material.

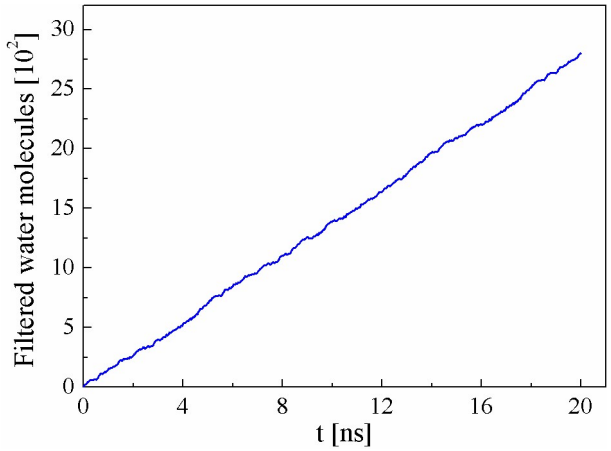

Fig. S3 The water fluxes in bilayer membrane under hydrostatic pressure of 50 MPa with 20 ns simulation.

7. The calculation of water permeability in bilayer membrane

As to the water permeability in bilayer membrane, using the four water flux obtained at 50, 100, 150, 200 MPa, we could fit a linear formula. The slope with a meaning of passed water number per ns per MPa through this membrane could be used to calculate the water permeability, it is 1172 L m^{-2} h^{-1} bar^{-1}.

8. The swelling of GO and 2D-CAP multilayer membrane

Here, the swelling performance of multilayer GO and bilayer 2D-CAP membranes were studied adopting molecular dynamics simulation. All membranes were allowed to relax freely in the simulation, which allowed the membrane to deform and accommodate the permeation of water molecules to swell them. The optimized GO (~10% oxidization degree) and 2D-CAP bilayer were merged with the water solution. We chose the all-atom optimized potentials for liquid simulations (OPLS-AA) to describe the functional groups (-C-OH, -C-O-C-) in GO and 2D-CAP sheets, which are widely used to cover essential many-body terms in interatomic interactions,[11] the other simulation details are same with that implemented in this paper. After several ns NVT simulation, these systems reach equilibrium, as shown in Fig. S2. As seen, a large number of water molecules permeate into the GO interlayer, resulting in swelling. The swelling causes the increase of interlayer spacing and lose the filtration ability for hydrated ions, which is a serious problem for seawater desalination. In the bilayer 2D-CAP membrane, though a large geometric deformation is found, no water was trapped in the interlayer, which is evident that no swelling occurs in the 2D-CAP membrane, a signature of robust desalination capability.

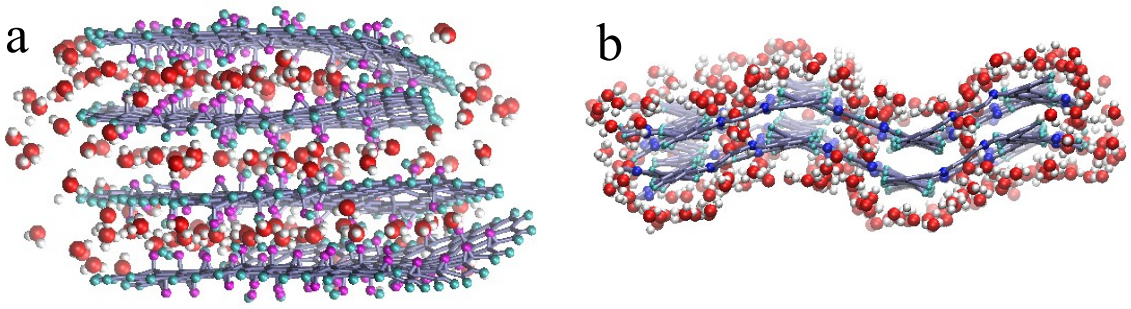

Fig. S4 Schematic showing the swelling of multilayer GO membrane (a) and bilayer 2D-CAP membrane (b) in water solution. Color codes: O_{wat}: red, H_{wat}: white, $O_{Hydroxyl}$ and O_{Epoxy}: magenta, $H_{Hydroxyl}$ and H_{edge}: cyan, C: iceblue.

9. The maps of water density in four membranes

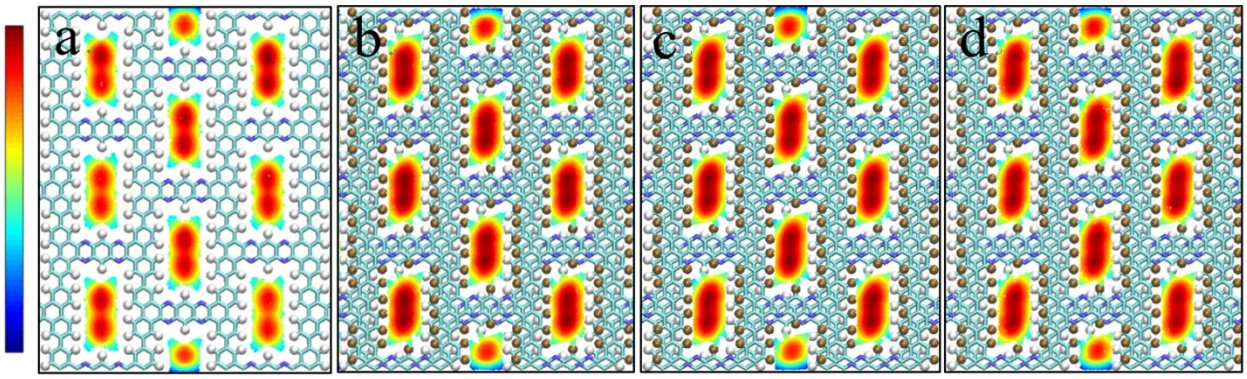

Fig. S5 The maps of water density in four membranes: (a) monolayer, (b) bilayer, (c) trilayer, (d) tetralayer.

10. The effect of electrostatic interaction on water flux

The electrostatic interaction between the partially charged hydrogen atom and the passing water molecules has two competing effects on water permeation. One is the enhancement effect that the electrostatic interaction increases the permeation rate of water molecules into pore. It is worth noting that the enhanced permeation rate is mainly contributed by the leftmost flake (entrance) near to the feeding box of the channel. The other is the reduction effect that the electrostatic sticking between the passing water and the partially charged rim atoms slows down water flow. Therefore, these two competing effects determine the water flux.

In all channels (mono-, bi-, tri-, and tetralayer), the enhancement effect has negligible difference as a function of thickness because it mainly contributed from the leftmost flake, while the reduction effect is determined by the channel length (layer number). In the case of monolayer, the single layer will exert small electrostatic sticking resistance to passing water molecules, yielding a high water flux. With the increase of layer number, every layer will exert sticking resistance on the passing water molecules, thus presenting firction to the water flow.

11. The calculation details for PMF profiles

In order to probe forces governing the ion transport across the channel of 2D-CAP, the potential

of mean forces (PMFs) for ions were studied (free energy). The PMFs were determined in umbrella sampling (US) calculations.[12-14] The reaction coordinate going along the center of the channel was partitioned into 14(monolayer), 17(bilayer), 20(trilayer), 23(tetralayer) windows of 1 Å widths, respectively. Confinement potentials were introduced in the form of harmonic restraints with a force constant of k = 1 kcal/(mol·Å^2),[15] and each window was run for 10 ns. The weighted histogram analysis method (WHAM)[15] was used to reconstruct the PMF. The PMF profiles of Na^+ and Cl^- ions in four membranes was considered.

PMF for water was determined using the average densities in equilibrium simulations using the fact that PMF(z) =-kTln(ρ(z)/ρ_o), where ρ(z), ρ_o is the water density at position of z and in bulk, respectively.[17]

References

[1] Zhang H., He X., Zhao M., et al. Tunable hydrogen separation in sp–sp^2 hybridized carbon membranes: a first-principles prediction. *J. Phys. Chem. C* **116**, 16634-16638 (2012).

[2] Frisch M. J., Trucks G. W., Schlegel H. B., et al. Gaussian 09, Revision A, Gaussian[J]. Inc., Wallingford CT, 2009.

[3] Chen Q., Yang X. Pyridinic nitrogen doped nanoporous graphene as desalination membrane: molecular simulation study. *J. Membrane Sci.* **496**, 108-117 (2015).

[4] Kou J., Zhou X., Lu H., et al. Graphyne as the membrane for water desalination. *Nanoscale* **6**, 1865-1870 (2014).

[5] Cohen-Tanugi, D., Grossman J. C. Water desalination across nanoporous graphene. *Nano Lett.*, **12**, 3602-3608 (2012).

[6] Abascal J. L. F., Vega C. A general purpose model for the condensed phases of water: TIP4P/2005. *J. Chem. Phys*. **123**, 234505 (2005).

[7] Müller-Plathe F. Local structure and dynamics in solvent-swollen polymers[J]. *Macromolecules*, **29**, 4782-4791 (1996).

[8] Jorgensen W. L., McDonald N. A. Development of an all-atom force field for heterocycles. Properties of liquid pyridine and diazenes. *J. Mol. Struc-Theochem*, **424**, 145-155 (1998).

[9] Barati Farimani A., Aluru N. R. Spatial diffusion of water in carbon nanotubes: from fiction to ballistic motion. *J. Phys. Chem. B* **115**, 12145-12149 (2011).

[10] Joung I. S., Cheatham T. E. Determination of alkali and halide monovalent ion parameters for use in explicitly solvated biomolecular simulations. *J. Phys. Chem. B* **112**, 9020-9041 (2008).

[11] Jorgensen W. L., Maxwell D. S., Tirado-Rives J. Development and Testing of the Opls All-Atom Force Field on Conformational Energetics and Properties of Organic Liquids. *J. Am. Chem. Soc.* **118**, 11225-11236 (1996).

[12] Torrie G. M., Valleau J. P., Nonphysical Sampling Distributions in Monte Carlo Free-Energy Estimation: Umbrella Sampling. *J. Comput. Phys.* **23**, 187-199 (1977).

[13] Kumar S., Rosenberg J. M., Bouzida D., Swendsen R. H., Kollman P. A. Multidimensional Free-Energy Calculations Using the Weighted Histogram Analysis Method. *J. Comput. Chem.* **16**, 1339-1350 (1995).

[14] Roux B. The Calculation of the Potential of Mean Force Using Computer Simulations. *Comput. Phys. Commun.* **91**, 275-282 (1995).

[15] Fiorin G., Klein M. L., Hénin J. Using collective variables to drive molecular dynamics simulations. *Mol. Phys.* **111**, 3345-3362 (2013).

[16] Andrec M. The Weighted Histogram Analysis Method (WHAM). Fynn, 2010.

[17] Corry B. Designing carbon nanotube membranes for efficient water desalination *J. Phys. Chem. B* **112**, 1427-1434 (2008).